Supplementary Information

5-Carboxy-8-hydroxyquinoline is a Broad Spectrum 2-Oxoglutarate Oxygenase Inhibitor which causes Iron Translocation

Richard J. Hopkinson,‡[a] Anthony Tumber,‡[b] Clarence Yapp,‡[b] Rasheduzzaman Chowdhury,‡[a] WeiShen Aik,[a] Ka Hing Che,[b,c] Xuan Shirley Li,[f] Jan B. L. Kristensen,[a,e] Oliver N. F. King,[a] Mun Chiang Chan,[a,d] Kar Kheng Yeoh,[a,d,§] Hwanho Choi,[a] Louise J. Walport,[a] Cyrille C. Thinnes,[a] Jacob T. Bush,[a] Clarisse Lejeune,[a] Anna M. Rydzik,[a] Nathan R. Rose,[a,f] Eleanor A. Bagg,[a] Michael A. McDonough,[a] Tobias Krojer,[b] Wyatt W. Yue,[2] Stanley S. Ng,[2,3] Lars Olsen,[5] Paul E. Brennan,[2] Udo Oppermann,[2,3] Susanne Muller-Knapp,[b] Robert J. Klose,[f] Peter J. Ratcliffe,[d] Christopher J. Schofield*[a] and Akane Kawamura*[a]

[a] Chemistry Research Laboratory, Department of Chemistry, University of Oxford, Mansfield Road, Oxford, OX1 3TA, U.K..

[b] Structural Genomics Consortium, University of Oxford, Headington, OX3 7DQ, U.K.

[c] Botnar Research Centre, Oxford Biomedical Research Unit, Oxford OX3 7LD, U.K..

[d] Henry Wellcome Building for Molecular Physiology, Department of Clinical Medicine, University of Oxford, Roosevelt Drive, Oxford OX3 7BN, U.K.

[e] Department of Medicinal Chemistry, Faculty of Pharmaceutical Sciences, University of Copenhagen, Universitetsparken 2, DK-2100 Copenhagen, Denmark.

[f] Epigenetic Regulation of Chromatin Function Group, Department of Biochemistry, University of Oxford, South Parks Road, Oxford, OX1 3QU, U.K.

§ Current address: School of Chemical Sciences, Universiti Sains Malaysia, 11800 USM Penang, Malaysia.

Corresponding Authors; christopher.schofield@chem.ox.ac.uk, akane.kawamura@chem.ox.ac.uk

‡ Authors contributed equally to the work.

Table S1. Rank Orders of inhibition for 5-carboxy-8-hydroxyquinoline (IOX1), *N*-oxalylglycine (NOG), 2,4-pyridine dicarboxylic acid (2,4-PDCA) and 4-carboxy-8-hydroxyquinoline (4C8HQ) against 2OG oxygenases. Near equal IC_{50} values are grouped. Where multiple IC_{50} values are present (see **Table 1** in Main Text), values derived from the same assay conditions were selected. 1 = most potent inhibitor.

2OG oxygenase	Rank Order of Inhibition			
	IOX1	NOG	2,4-PDCA	4C8HQ
PHD2	2	1	3	4
FIH	3=	1=	1=	3=
KDM4A (JMJD2A)	1	4	2=	2=
KDM4C (JMJD2C)	1	4	2=	2=
KDM4D (JMJD2D)	1	4	2	3
KDM4E (JMJD2E)	1	4	2=	2=
KDM3A (JMJD1A)	1	2	3	4
KDM6B (JMJD3)	1	2	4	3
KDM6A (UTX)	1	3	4	2
KDM2A (FBXL11)	2=	4	1	2=
PHF8	1=	4	3	1=
KDM5C (JARID1C)	3=	2	1	3=
BBOX1	4	3	1	2
AlkB	3=	2	1	3=
Mean Rank Order	1.78	2.85	2.14	2.57

Table S2. Metal Coordination data from crystal structures for AlkB, FIH, KDM4A (JMJD2A) and KDM6B (JMJD3) showing interatomic distances between metal and the H(His-1)XD/E...H(His-2) protein ligands. Structures with IOX1 are highlighted in bold. Increased interatomic distances between the metal and His-2 observed with IOX1/GSK-J1 are highlighted in red. Two inhibitor molecules were observed to be bound in the active site in the case of *N*-3-dihydroxybenzamide - here this structure is likely not representative.

Protein	PDB	Ref	Metal	Ligand(s)	Resol. Å	His-1 Å	Asp/ Glu O1 Å	Asp/ Glu O2 Å	His -2 Å
AlkB	**4JHT**	**Current**	**Mn^{II}**	**IOX1**	**1.2**	**2.2**	**2.1**	**3.5**	**2.4**
	3I3Q	[1]	Mn^{II}	2OG,	1.4	2.2	2.2	3.4	2.2
	2FDG	[2]	Fe^{II}	Succinate, TmAT	2.2	2.3	2.0	2.8	2.2
	2FDJ	[2]	Fe^{II}	Succinate	2.1	2.2	2.3	3.5	2.3
	3BIE	[3]	Mn^{II}	2OG, DNA	1.7	2.2	2.2	3.4	2.2
FIH	**3OD4**	**Current**	**Zn^{II}**	**IOX1**	**2.2**	**2.2**	**2.0**	**3.0**	**3.5**
	4BIO	**Current**	**Fe^{II}**	**IOX1**	**2.5**	**2.2**	**2.4**	**2.8**	**3.6**
	1H2K	[4]	Fe^{II}	NOG, HIF peptide	2.2	2.1	2.1	3.4	2.1
	1H2M	[4]	Zn^{II}	NOG, HIF peptide	2.5	2.0	2.1	3.4	2.0
	1YCI	[5]	Fe^{II}	*N*-oxalyl-D-phenylalanine	2.7	2.3	2.2	3.6	2.4
	2CGO	[6]	Fe^{II}	Fumarate	2.4	2.3	1.9	3.3	2.3
	2CGN	[6]	Fe^{II}	Succinate	2.5	2.2	2.0	3.2	2.4
	2W0X	[7]	Fe^{II}	2,4-PDCA	2.1	2.3	2.1	3.4	2.4
	2WA4	[7]	Fe^{II}	*N*,3-dihydroxybenzamide	2.5	2.2	5.4	7.0	2.3
	2WA3	[7]	Fe^{II}	3-hydroxyphenyl(oxo)acetic acid	2.5	2.3	2.1	3.3	2.3
KDM4A	**3NJY**	**[8]**	**Ni^{II}**	**IOX1**	**2.6**	**2.4**	**2.2**	**2.7**	**3.6**
	4BIS	Current	Ni^{II}	4C8HQ	2.5	2.3	2.1	3.5	2.3
	2OX0	[9]	Ni^{II}	NOG, H3K9me2	2.0	2.2	2.2	3.4	2.2
	2OT7	[9]	Ni^{II}	NOG, H3K9me1	2.1	2.3	2.1	3.5	2.1
	2OS2	[9]	Ni^{II}	NOG, H3K36me3	2.3	2.3	2.1	3.5	2.1
	2OQ7	[9]	Ni^{II}	NOG	2.2	2.3	2.2	3.5	1.9
	2OQ6	[9]	Ni^{II}	NOG, H3K9me3	2	2.1	2.1	3.5	2.1
	2Q8E	[10]	Ni^{II}	NOG, H3K36me3	2.1	2.1	2.1	3.5	1.9
	2Q8D	[10]	Ni^{II}	succinate, H3K36me2	2.3	2.3	2.2	3.4	2.2
	2PXJ	[11]	Fe^{II}	NOG, H3K36me1	2	2.1	2.4	3.5	2.2
	2P5B	[11]	Fe^{II}	NOG, H3K36me3	2.1	2.2	2.1	3.4	2.1
	2VD7	[12]	Ni^{II}	2,4-PDCA	2.3	2.2	2.2	3.4	2.2
	2WWJ	[13]	Ni^{II}	*O*-benzyl-*N*-(carboxycarbonyl)-D-tyrosine	2.6	2.3	2.0	3.4	2.1
KDM6B	**2XXZ**	**Current**	**Ni^{II}**	**IOX1**	**1.8**	**2.1**	**2.1**	**3.3**	**3.7**
	2XUE	[14]	Fe	2OG	2.0	2.1	1.9	3.7	2.1
	4ASK	[14]	Co^{II}	GSK-J1	1.9	2.2	2.2	3.4	3.9

Table S3. Data Collection and Refinement Statistics Table.

	AlkB.Mn.IOX1	FIH.Zn.IOX1	FIH.Fe.IOX1	KDM4A.Ni.4C8HQ	KDM6B.Ni.IOX1
PDB acquisition codes	4JHT	3OD4	4BIO	4BIS	2XXZ
Data collection					
Beamline (Wavelength, Å)	DLS I04 (0.9763)	DLS I04 (0.9763)	DLS I03 (0.9794)	DLS I04-1 (0.9163)	DLS I02 (0.9795)
Detector	ADSC Q315r	ADSC Q315r	Pilatus 6M	Pilatus 6M	ADSC Q315r
Data processing	HKL2000[15]	MOSFLM,[18] SCALA[17]	XDS,[16] SCALA[17]	XDS,[16] SCALA[17]	MOSFLM,[18] SCALA[17]
Space group	*P*1	$P4_12_12$	$P4_12_12$	$P2_12_12$	$P2_12_12_1$
Cell dimensions					
a, *b*, *c* (Å)	36.84, 38.85, 40.45	86.40, 86.40, 147.20	86.71, 86.71, 147.1	100.69, 150.15, 57.45	56.76, 71.43, 159.70
α, *β*, *γ* (°)	77.62, 75.01, 66.10	90, 90, 90	90, 90, 90	90, 90, 90	90, 90, 90
No. reflections	60068 (5299)*	28069	21369 (3031)*	31126 (3048)*	61104
Resolution (Å)	38.77 – 1.18 (1.22 – 1.18)*	38.64 – 2.20 (2.32 – 2.20)*	56.59 – 2.45 (2.54 – 2.45)*	60.19 – 2.49 (2.58 – 2.49)*	29.16 – 1.8 (1.9 – 1.8)*
R_{sym} or R_{merge}**	0.080 (0.333)*	0.086 (0.69)*	0.086 (0.802)*	0.1 (0.787)*	0.1 (0.96)*
$I/\sigma I$	18.45 (3.83)*	13.4 (1.1)*	12.8 (2.2)*	11.8 (2.2)*	8.5 (2.0)*
Completeness (%)	93.30 (85.70)*	99.9 (100)*	99.3 (100)*	99.8 (99.9)*	99.9 (100)*
Redundancy	4.1 (3.1)*	8.9 (9.2)*	7.1 (7.4)*	5.5 (5.8)*	4.8 (4.8)*
Wilson *B* value (Å^2)	13.80	44.5	54.5	30.9	24.0
Refinement					
R_{work}/ R_{free}‡	0.159 / 0.166	0.176 / 0.212	0.201 / 0.234	0.193 / 0.224	0.184 / 0.216
No. atoms					
-Protein (A/B)	1610	2848	2759	2785/ 2807	2400/ 2311
-IOX1/4C8HQ	14	14	14	14/ 14	14/ 14
-Water	269	146	123	128/ 135	164/ 155
B-factors (Å^2)					
-Protein	19.90	62.67	59.52	40.47/ 40.53	28.58 / 34.92
-IOX1/4C8HQ	15.14	44.64	46.80	38.05/ 43.30	17.38 / 22.58
-Water	32.70	57.28	51.79	36.34/ 37.30	19.66/ 20.18
R.m.s deviations					
-Bond lengths (Å)	0.009	0.01	0.011	0.007	0.013
-Bond angles (°)	1.25	1.17	1.39	1.26	1.35

*Highest resolution shell shown in parenthesis.

**$R_{sym} = \sum|I-\langle I\rangle|/\sum I$, where I is the intensity of an individual measurement and $\langle I\rangle$ is the average intensity from multiple observations.

‡$R_{factor} = \sum_{hkl}||F_{obs}(hkl)| - k\,|F_{calc}(hkl)||/\sum_{hkl}|F_{obs}(hkl)|$ for the working set of reflections; R_{free} is the R_{factor} for ~5% of the reflections excluded from refinement.

AlkB

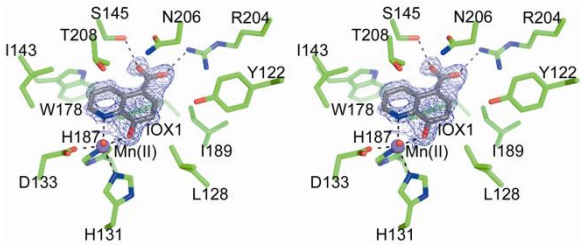

FIH

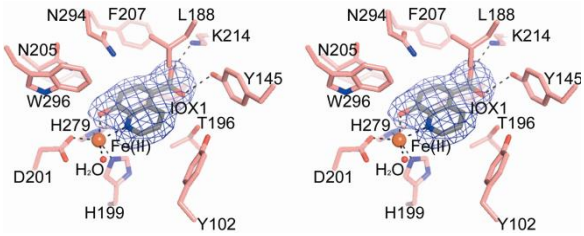

KDM4A

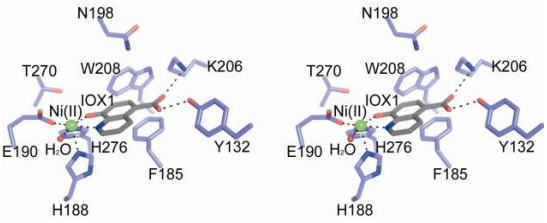

KDM6B

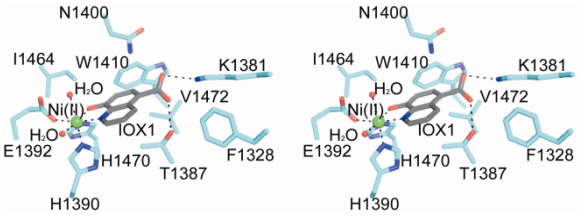

Figure S1. Stereo-views from crystal structures of IOX1 bound to AlkB (PDB ID: 4JHT), FIH (PDB ID: 4BIO), KDM4A (JMJD2A, PDB ID: 3NJY)[8] and KDM6B (JMJD3, PDB ID: 2XXZ). The electron density maps (*Fo*-*Fc* OMIT) are for IOX1 contoured to 6 and 3σ in the AlkB and FIH complex structures respectively. Dotted lines indicate apparent hydrogen-bonds / polar interactions.

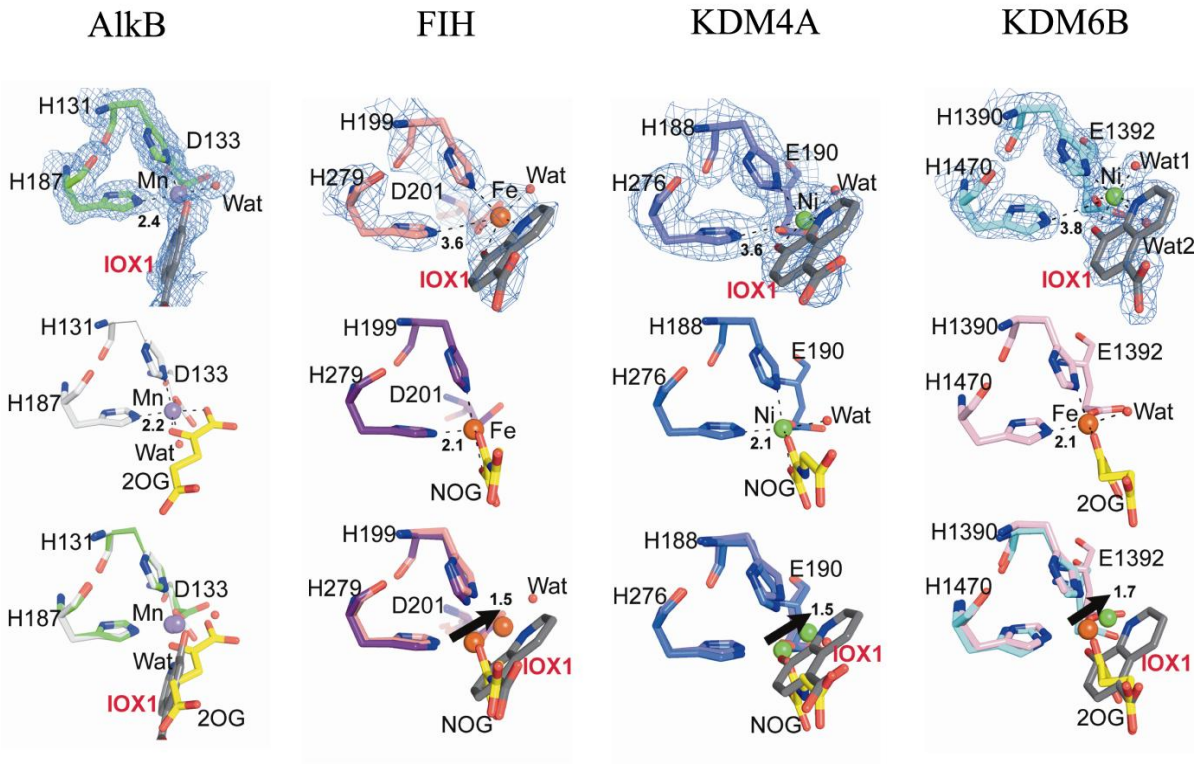

Figure S2. Views from crystal structures of IOX1 bound to AlkB (PDB ID: 4JHT), FIH (PDB ID: 4BIO), KDM4A (JMJD2A, PDB ID: 3NJY)[8] and KDM6B (JMJD3, PDB ID: 2XXZ), overlaid with structures with 2OG/NOG. Metal translocation is highlighted.

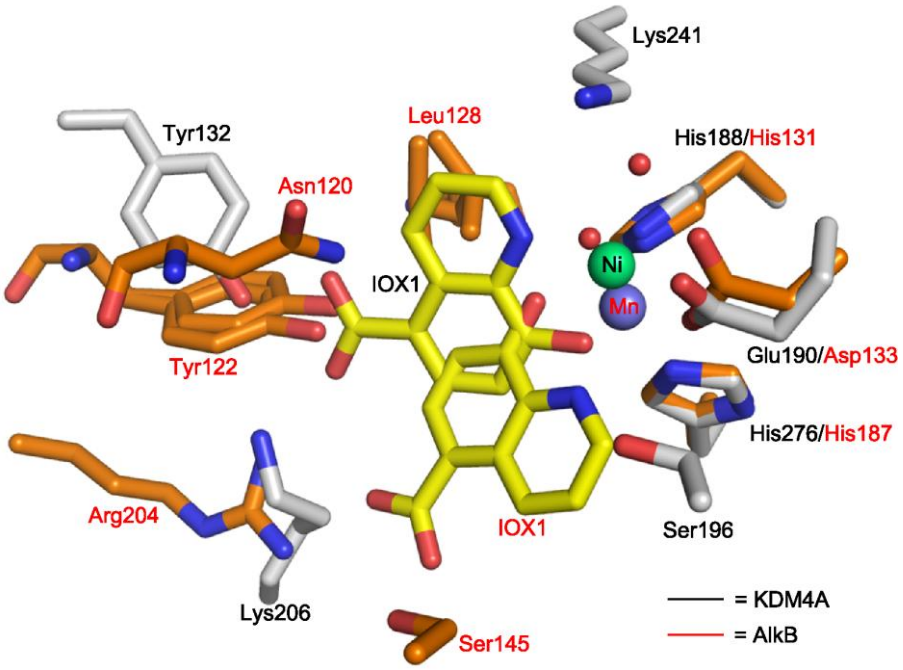

Figure S3. Views from crystal structures of IOX1 bound to KDM4A (JMJD2A, PDB ID: 3NJY)[8] and AlkB (PDB ID: 4JHT). Red labels highlight residues from the AlkB complex structure. Two conformations were observed for both Tyr122 and Leu128 in the AlkB structure, which is likely due to the partial occupancy (50 %) of IOX1 in the active site.

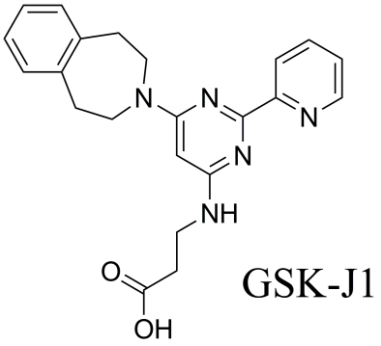

Figure S4. Structure of GSK-J1.

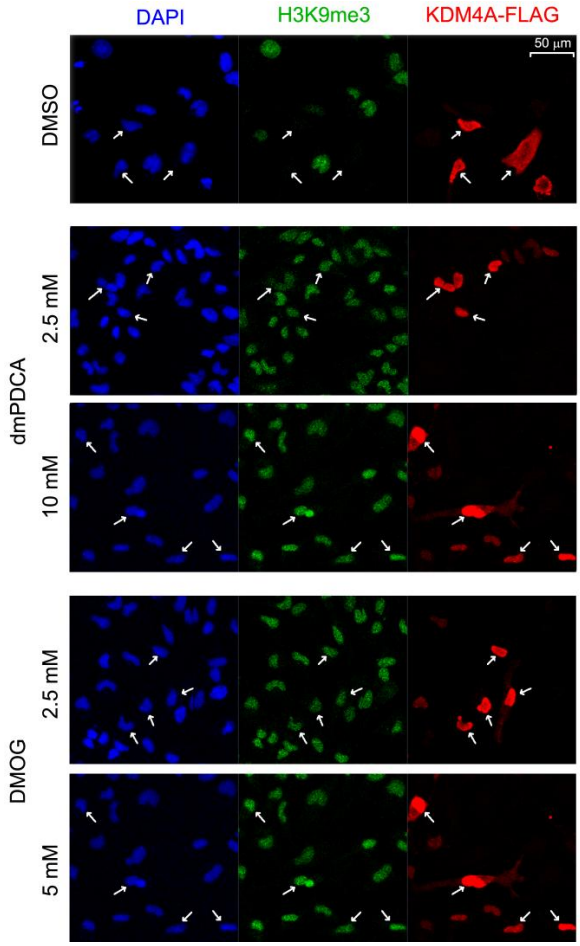

Figure S5. Inhibition of KDM4A in HeLa cells by dmPDCA and DMOG.

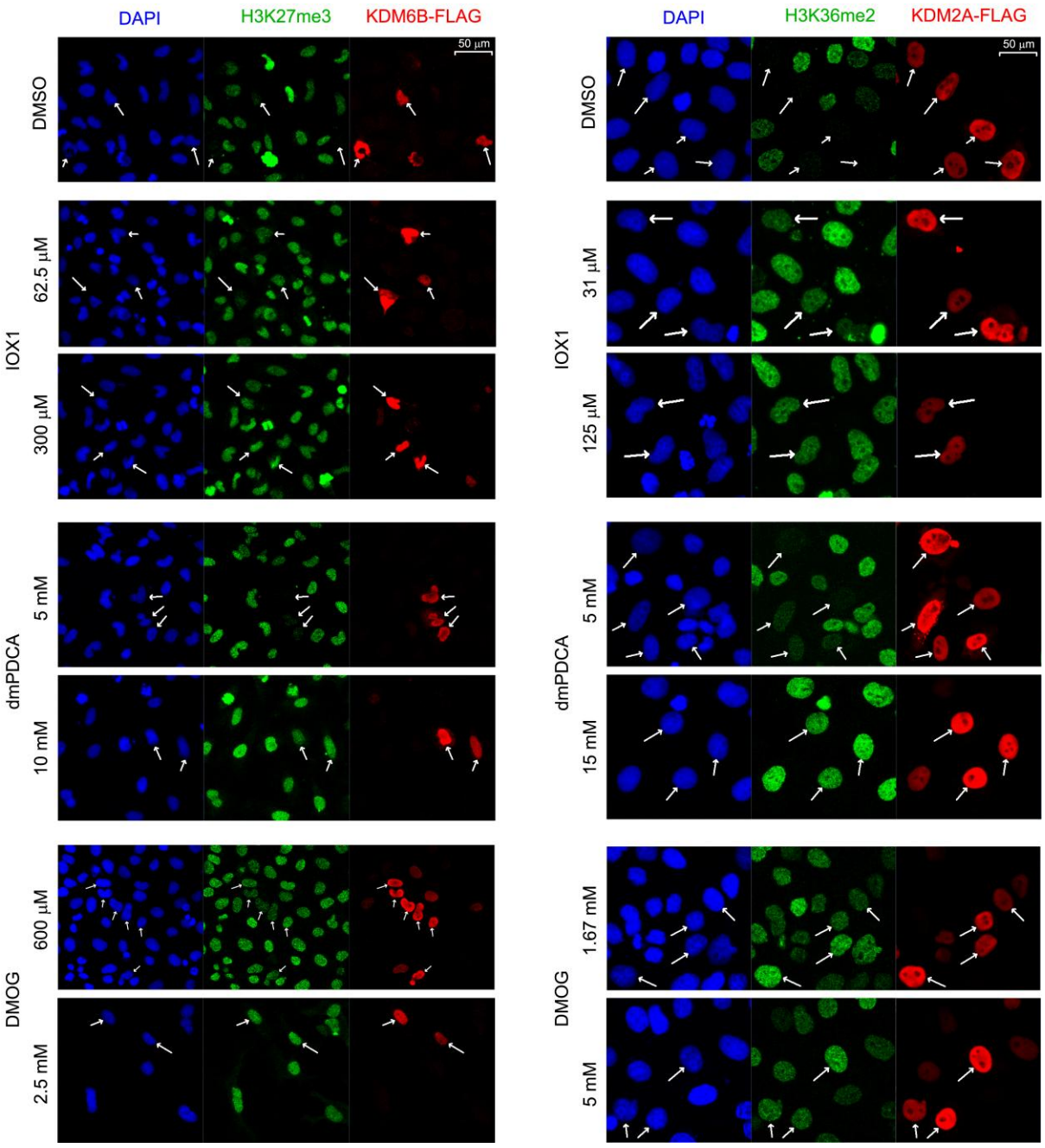

Figure S6. Inhibition of KDM6B (left) and KDM2A (right) in HeLa cells by IOX1, dmPDCA and DMOG.

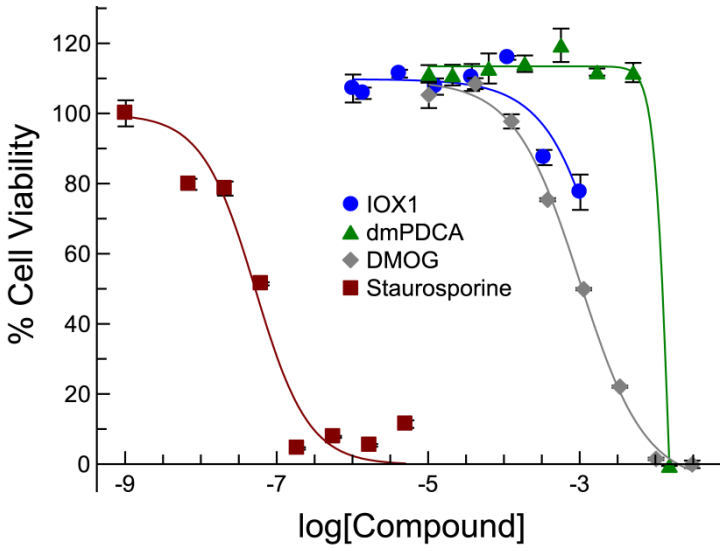

Figure S7. Cytotoxicity of IOX1, dmPDCA, DMOG and Staurosporine in HeLa cells.

Recombinant Protein Production

PHD2,[19] FIH,[20] KDM4A,[9] KDM4C,[21] KDM4D,[21] KDM4E,[12] KDM3A,[22] KDM6B,[22] KDM6A,[23] KDM2A,[24] PHF8,[22] KDM5C[22] and AlkB[25] were heterologously expressed in *E. coli* as described. BBOX1 was expressed in *Baculovirus* as described.[26]

In Vitro Inhibition Assays

In vitro inhibition studies were carried using either AlphaScreen assays (PHD2, KDM4A/C/D/E, KDM3A, KDM6A/B, KDM2A, PHF8 and KDM5C),[22] formaldehyde dehydrogenase coupled assays (AlkB,[21] KDM6A), a fluoride detection based assay (BBOX1),[27] and MALDI-MS based assays (FIH, PHF8).

AlphaScreen Assays

AlphaScreen (Amplified Luminescence Proximity Homogeneous Assay) inhibition assays were carried out as previously reported.[22, 28] Assays were carried out in 384-well plates using white Proxiplates (Perkin Elmer). Hydroxyethyl-piperazine-ethane sulfonic acid (HEPES) buffer was purchased from Apollo Scientific. Ferrous ammonium sulphate (FAS) was made fresh in 20 mM HCl to a concentration of 400 mM and then diluted to 1 mM in deionised water. Bovine serum albumin (BSA) was free of fatty acid and globulin (Sigma A7030). AlphaScreen General IgG detection kit was purchased from Perkin Elmer. Biotinylated peptides were synthesised in house or purchased from GLS China (Shanghai, China) or Pepceuticals (Leicestershire, U.K.). Antibodies against peptide products were as previously reported. All other reagents were from Sigma-Aldrich. Protocols for the KDM2A, KDM3A, KDM4A/C, KDM5C, KDM6B and PHF8 assays were as previously reported. The KDM6A inhibition assay was carried out in a total volume of 10 µL containing KDM6A (200 nM), 2OG (10 µM), ferrous iron (10 µM), Biotin-H3(14-34)K27me3 peptide (250 nM), non-biotinylated H3(14-34)K27me3 peptide (1 µM) and inhibitor (1 % DMSO in final reaction). The reaction was stopped after 1 hour by addition of EDTA (30 mM) and the product peptide (biotinylated) was detected by addition of 5 µL of AlphaScreen donor and acceptor beads that

previously had been incubated with the anti-dimethyl-Histone H3 (Lys27) antibody (Millipore 07-452). The sample was then left for 1 hour before analysis in a BMG Labtech Pherastar FS plate reader. Data were normalised to the no enzyme control and IC_{50} values calculated from nonlinear regression curve fits using GraphPad Prism 5.

Formaldehyde Dehydrogenase (FDH) Coupled Assays

K_M^{app} values for 2OG with KDM6A and AlkB were determined using FDH coupled assays. Samples (total volume 25 μL) were monitored over initial time points as described, and kinetic parameters were determined by plotting the Michaelis-Menten equation using GraphPad Prism 5. For KDM6A, samples contained KDM6A (2.5 μM), 2OG, non-biotinylated H3(14-34)K27me3 peptide (500 μM), ferrous iron (50 μM), NAD (2 mM) and formaldehyde dehydrogenase (0.0125 units) in 50 mM HEPES 50 mM NaCl pH 7.5 buffer. AlkB samples contained AlkB (2 μM), 2OG, oligonucleotide containing 1-methyladenine (20 μM, sequence GC-1meA-AGGTCCCGTAGTGCG, ATD Bio, U.K.) ascorbate (100 μM), ferrous iron (10 μM), NAD (500 μM) and formaldehyde dehydrogenase (0.025 units) in 50 mM HEPES buffer pH 7.5. For AlkB inhibition assays, samples also contained inhibitor (2.5 μL). Enzyme, FDH and inhibitor were preincubated for 15 minutes prior to addition of other reagents. Data were normalised to the no enzyme control and IC_{50} values calculated from nonlinear regression curve fits using GraphPad Prism 5.

MALDI-TOF Assays

Inhibition assays for FIH and PHF8 were carried out as follows. For FIH inhibition, samples (total volume 10 μL) containing FIH (1 μM), consensus ankyrin peptide (sequence HLEVVKLLLEAGADVNAQDK, 100 μM), 2OG (10 μM), ascorbate (100 μM), ferrous iron (10 μM) and inhibitor in 50 mM HEPES pH 7.5 buffer, were incubated for 5 minutes before quenching with MeOH (20 μL). Enzyme, ascorbate, ferrous iron and inhibitor were pre-incubated for 15 minutes prior to addition of substrate and 2OG. After quenching, aliquots of each sample (1 μL) were then mixed with 1 μL of 1 mg/mL α-cyano-4-hydroxycinnamic acid and assessed by matrix-assisted laser desorption/ionization-time of flight (MALDI-TOF) Mass Spectrometry (Micromass). PHF8 samples (total volume 10 μL) contained PHF8 (2 μM), 2OG (15 μM), non-biotinylated H3(1-14)K4me3K9me2 peptide (10 μM), ascorbate (100 μM), ferrous iron (10 μM) and inhibitor in 100 mM HEPES 500 mM NaCl pH 7.5 buffer. Reactions were quenched after 10 minutes using MeOH (20 μL) before MALDI-MS analysis. Data were normalised to the no enzyme control and IC_{50} values calculated from nonlinear regression curve fits using GraphPad Prism 5.

Crystallography

Recombinant forms of AlkB,[25] FIH,[20] KDM4A[9] and KDM6B[14] were expressed in *Escherichia coli* BL21 (DE3) and purified as reported. Crystals of AlkB, FIH, KDM4A and KDM6B in complex with IOX1/4C8HQ were grown in sitting drops under conditions described in **Table S4**. In general, crystals were cryoprotected by transferring to a solution of mother liquor supplemented with 15-25 % v/v glycerol before being cyro-cooled in liquid N_2. Data were collected from single crystals at 100K using synchrotron radiation at the Diamond Light Source (DLS) beamlines. The data were processed as outlined in **Table S3**. Structures of AlkB, FIH and KDM4A were solved by molecular replacement using PHASER[29] or by isomorphous replacement using PHENIX[30]; PDB ID 1H2K (for FIH), 3T4V

(for AlkB), 2OX0 (for KDM4A) were used as initial search models. A single wavelength anomalous dispersion (SAD) dataset was collected for KDM6B.IOX1 seleno-methionine derivatized crystal. The structure of KDM6B.IOX1 complex was solved as described.[14] Iterative rounds of model building and refinement using COOT[31] and PHENIX[30] and/or CNS[32] were performed until the decreasing R and R_{free} no longer converged. All residues were in acceptable regions of Ramachandran plots as calculated by MolProbity.[33] Data collection and refinement statistics are shown in **Table S3**.

Table S4. Crystallization conditions

	AlkB.Mn.IOX1	FIH.Zn.IOX1	FIH.Fe.IOX1	KDM4A.Ni.4C8HQ	KDM6B.Ni.IOX1
Sample composition	AlkB (0.44 mM in 50 mM Hepes pH 7.5) + $MnCl_2$ (1 mM) + IOX1 (1 mM)	FIH (0.25 mM in 10 mM HEPES pH 7.5, 200 mM NaCl) + IOX1 (0.25 mM)	FIH (0.25 mM in 50 mM Tris pH 7.5) + $FeCl_2$ (1 mM) + IOX1 (1 mM)	KDM4A (0.25 mM in 10 mM HEPES pH 7.5, 200 mM NaCl, 5% glycerol) + Ni (1 mM) + 4C8HQ (1 mM)	KDM6B (0.25 mM in 20 mM Tris pH 8.0, 150 mM NaCl, 5 % glycerol, 0.5 mM TCEP) + $Fe(NH_4)_2(SO_4)_2$ (10 μM) + IOX1 (2 mM)
Crystallization condition	0.1M HEPES pH 7.5, 0.264 M NaCl, 23% w/v PEG 3350	0.1M HEPES pH 7.5, 1.75 M ammonium sulfate, 2% w/v PEG 400, 0.002 M $ZnCl_2$	0.1M HEPES pH 7.5, 1.2 M ammonium sulfate, 3% w/v PEG 400, 0.001 M $FeCl_2$	0.1 M Bis-Tris propane pH 7.5, 0.02 M sodium/potassium phosphate, 20 % w/v PEG 3350	0.1 M Tris pH 8.0, 37.5 % 2-Methyl-2,4-pentanediol, PEG 1000, 0.03 M $MgCl_2$, 0.03 M $CaCl_2$
Vapor diffusion conditions	Sitting drop, protein-to-well ratio, 1:1, 293K	Sitting drop, protein-to-well ratio, 1:1, 293K	Sitting drop, near anaerobic (PO_2 <0.1 ppm), protein-to-well ratio, 1:1, 293K	Sitting drop, protein-to-well ratio, 1:1, 277K	Sitting drop, protein-to-well ratio, 1:1, 293K

Theory and Computational Methods

Potential energy landscapes of IOX1 and 4C8HQ bound within the active site of KDM4A (PDB IDs: 3NJY and 4BIS respectively) were analyzed via the optimization of energy calculations using Schrödinger 9.0. Structure frameworks of the binding pockets are shown in **Figure S8**. In each model, the chelating Ni(II) ion was replaced with Fe(II) to represent the biological systems.

Quantum chemical calculations were carried out using density functional calculations with the 6-31G* basis set for all atoms. The M06 hybrid density functional was employed for all calculations.[34] This functional consists of meta-hybrid hybrid GGA DFT functional[35] and M06 family functionals which are parametrized including both transition metals and non-metals.

Energy values for the KDM4A-IOX1 complex, the KDM4A-4C8HQ complex, KDM4A and the ligands respectively were calculated using energy minimization methods. The calculated energy difference between the KDM4A-IOX1 complex and the corresponding KDM4A-4C8HQ complex (**Equation S1**) was -7.98 Kcal mol^{-1}.

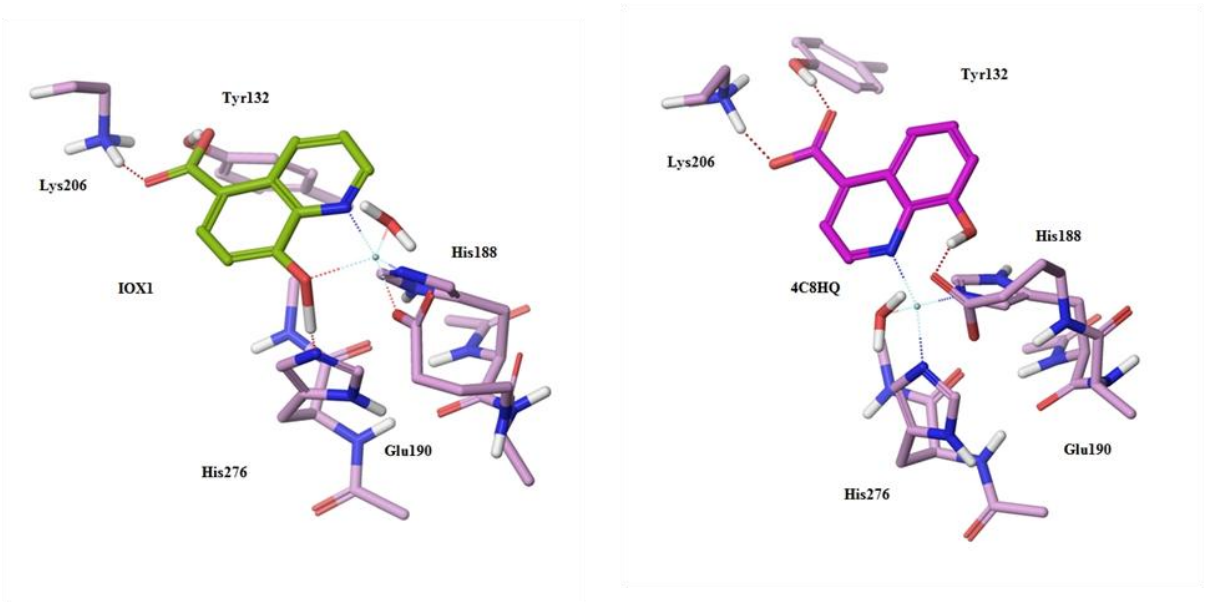

Figure S8. Structure frameworks used for potential energy calculations of IOX1 (left) and 4C8HQ (right) binding to KDM4A, as derived from crystal structures (PDB IDs: 3NJY[8] and 4BIS respectively).

$$\Delta E^{\,difference}_{IOX1\text{-}4C8HQ} = \Delta E_{KDM4A\ IOX1} - \Delta E_{KDM4A\ 4C8HQ}$$

$$= [E^{\,complex}_{KDM4A\ IOX1} - (E_{KDM4A} + E_{IOX1})] - [E^{\,complex}_{KDM4A\ 4C8HQ} - (E_{KDM4A} + E_{4C8HQ})]$$

Equation S1. Determination of the energy difference between IOX1 and 4C8HQ binding to KDM4A.

Cell-Based Assays

Constructs

Flag-tagged full length KDM4A[8] and KDM6B[14] were used for immunofluorescence assays. Overexpression of wild type KDM2A resulted in perinucleolar foci and incomplete demethylation of histone 3 lysine-36Me2 throughout the nucleus. To distribute KDM2A and therefore its enzymatic activity more evenly throughout the nucleus we overexpressed KDM2A with a point mutation in the CXXC domain, K601A which abrogates KDM2A binding to unmethylated CpG dinucleotides.[36]

Cell culture

HeLa cells were cultured at 37 °C and 5 % CO_2 in RPMI 1640 medium (Sigma Aldrich) and supplemented with 10 % FCS (Invitrogen), 1 % Glutamax (Invitrogen), and 1 % Penicillin-streptomycin (Lonza). HeLa cells were seeded into 96-well clear-bottom optical-grade plates (BD Biosciences) at 8000 cells per well and allowed to settle overnight. The next day, the

medium was changed to antibiotics-free medium. For each well, 0.1 μg of plasmid and 0.25 μL of Lipofectamine 2000 (Invitrogen) were each incubated in 25 μL of OptiMEM (Invitrogen) for 5 minutes at room temperature. The two solutions were then combined and mixed gently but thoroughly and incubated for 20 minutes at room temperature. The mixture was then added to the cells. Four hours later, the medium was changed to regular culture medium with antibiotics and dosed with varying concentrations of compound. The amount of DMSO in each well was kept constant throughout the plate. The cells were incubated for a further 24 hours before being fixed for immunostaining.

Immunostaining

Cells were fixed in 4 % formaldehyde for 20 minutes, permeabilised in 0.5 % Triton-X 100 for 6-10 minutes, and blocked in 3 % FCS for 1 hour with a PBS wash in between each step. The primary antibodies were then added to the cells in blocking solution and left overnight. The next day, cells were washed 3 times in PBS, incubated with secondary antibodies for 1 hour, rinsed 3 times in PBS again, and counterstained with DAPI before imaging.

Imaging

Immunostained cells were imaged on the BD Pathway high content analyser (BD Biosciences). Briefly, the exposure time for DAPI, Alexafluor 488 and Alexafluor 568 was set up so as to utilise the entire 12-bit dynamic range. The system's autofocus and montage capture features were employed so as to automatically obtain multiple sharp images for each well, thus, increasing the sample size. After image acquisition, the data was imported and analysed in Attovision (BD Biosciences). Measurement of the fluorescence intensity of the Flag-tag and histone modification staining was restricted to the nucleus of each cell. The nuclei were automatically identified by DAPI staining. Cells expressing low amounts of the exogenous demethylase, where Flag-tag staining was dim, were omitted from analysis. Finally, the average intensity of the histone modification staining for the remaining cells in each well was exported to BD IDE (BD Biosciences) and Prism 5 (Graphpad) for plotting.

Chemical Synthesis

N-oxalylglycine (NOG) and dimethyloxalylglycine (DMOG) were synthesised as reported.[37] 2,4-pyridinedicarboxylic acid (2,4-PDCA) was purchased from Aldrich. Dimethyl-2,4-pyridinedicarboxylate (dmPDCA) was synthesised from 2,4-PDCA as reported.[38] 5-carboxy-8-hydroxyquinoline (IOX1) and 4-carboxy-8-hydroxyquinoline were synthesised as described below. Reagents and solvents were from Aldrich. TLC monitoring was performed using precoated aluminium-backed plates (Merck, silica 60 F254). Melting points were determined using a Leica Galen III hot-stage melting point apparatus and microscope. Infrared spectra were recorded on a Bruker Tensor 27 FT-IR spectrometer. NMR spectra were acquired using a Bruker DPX400 NMR spectrometer. Chemical shifts (δ) are given in ppm, and the multiplicities are given as singlet (s), doublet (d), triplet (t), quartet (q), multiplet (m), broad (br). Coupling constants *J* are given in Hz (± 0.5 Hz). High resolution mass spectra (HRMS) were recorded using a Bruker MicroTOF spectrometer.

5-carboxy-8-hydroxyquinoline (IOX1)

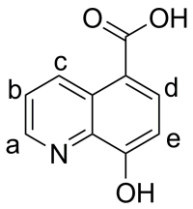

Acrolein (0.65 mL, 9.73 mmol) was added dropwise to a refluxing solution of 3-amino-4-hydroxybenzoic acid (1.00 g, 6.53 mmol) in 6N HCl (15 mL) and stirred at reflux for 2 h. The reaction mixture was cooled to r.t., diluted with water (15 mL), adjusted to pH 8 with aqueous ammonia and filtered. The filtrate was acidified to pH 4 with acetic acid and the resulting precipitate isolated by filtration and dried under vacuum. Purification by reverse phase chromatography afforded the product (563 mgs, 46%) as a pale brown powder. mp 275-277 °C (dec) [lit. mp 278-280 °C]; δ_H (200 MHz, DMSO-d_6) 9.49 (1 H, dd, J = 9.0, 1.0 Hz, H_a), 8.93 (1 H, m, H_c), 8.27 (1 H, d, J = 8.0 Hz, H_e), 7.71 (1 H, dd, J = 9.0, 4.0 Hz, H_b), 7.14 (1 H, d, J = 8.0 Hz, H_d); δ_C (100 MHz, DMSO-d_6) 168.1 (*C*=O), 158.3, 148.6, 138.6, 137.9, 133.9, 128.5, 128.5, 123.8, 116.8, 110.6;

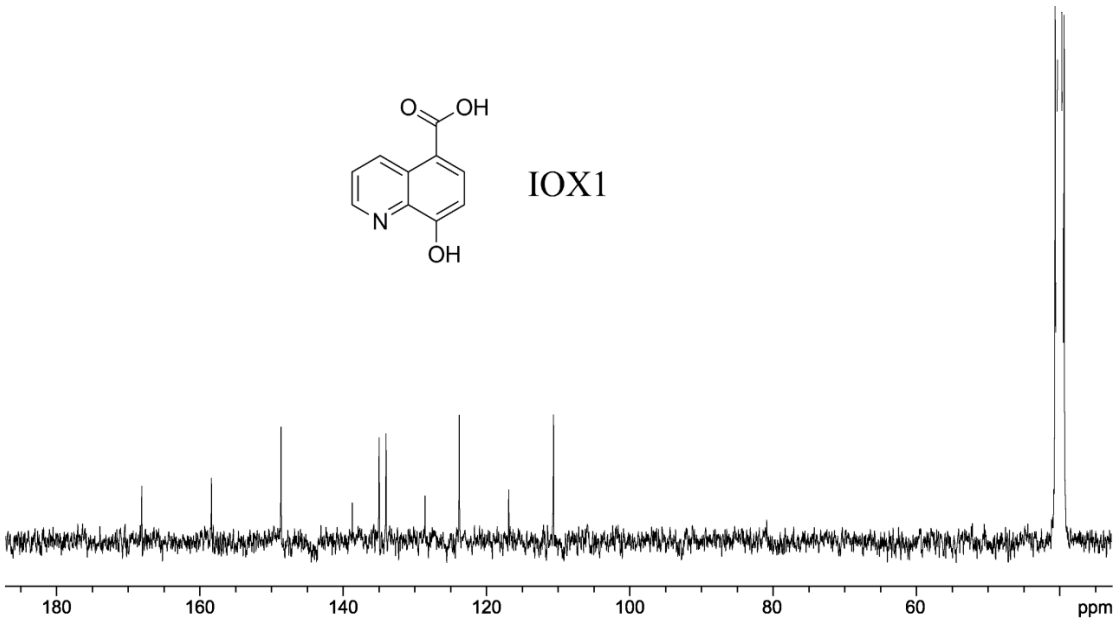

4-Carboxy-8-Sulfoquinoline

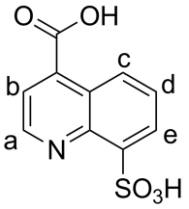

Fuming sulphuric acid (65 % SO_3, 1 mL) was added dropwise to 4-quinolinecarboxylic acid (1 g, 5.68 mmol) inside a 10 mL microwave vial. The vial was sealed and the reaction mixture heated at 200 °C in a sand bath for 2 h. The mixture was left to cool down to room

temperature and water (5 mL) was added dropwise. The black residue was triturated with water until formation of a homogenous white powder occurred. The powder was collected by filtration and dried under reduced pressure to give the product (886 mg, 61 %) as a white powder. mp > 300 °C [lit. mp > 300 °C]; ν_{max}/cm^{-1} 1721 (C=O); δ_H (400 MHz, DMSO-d_6) 9.50 (1 H, d, J = 5.5 Hz, H_a), 8.82 (1 H, d, J = 8.5 Hz, H_e), 8.49 (1 H, d, J = 7.5 Hz, H_c), 8.43 (1 H, d, J = 5.5 Hz, H_b) 8.05 (1 H, dd, J = 8.5, 7.5 Hz, H_e); δ_C (100 MHz, DMSO-d_6) 166.5 (*C*=O), 148.5, 146.9, 138.8, 135.2, 133.3, 130.9, 129.1, 126.7, 123.5; *m*/*z* (ESI$^-$) 252 ([M-H]$^-$); HRMS (ESI$^+$) $C_{10}H_7NNaO_2S$, ([M+Na]$^+$) requires 275.9937; found 275.9940.

4-carboxy-8-hydroxyquinoline (4C8HQ)

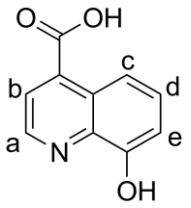

8-Sulfoquinoline-4-carboxylic acid (1 g, 3.95 mmol) was dissolved in a solution of potassium hydroxide (5 g, 89.3 mmol) in water. The solvent was evaporated under reduced pressure. The residue was heated above 300 °C with a heat gun until a colour change from off-white to dark yellow occurred. The residue was left to cool to room temperature and dissolved in water (200 mL). The pH was adjusted to 4.5 with aqueous hydrochloric acid and the solution was extracted with ethyl acetate (500 mL) three times. The combined organic layers were combined and dried over anhydrous Na_2SO_4 and the solvent was evaporated to give 4C8HQ (542 mg, 73 %) as a yellow solid. mp 259 °C [lit. mp 259 °C]; ν_{max}/cm^{-1} 2539 (O-H); δ_H (400 MHz, DMSO-d_6) 8.96 (1 H, d, J=4.5 Hz, H_a), 8.07 (1 H, d, J=8.0 Hz, H_e), 7.93 (1 H, d, J=4.5 Hz, H_b), 7.54 (1 H, t, J=8.0 Hz, H_d), 7.15 (1 H, d, J=8.0 Hz, H_c); δ_C (100 MHz, DMSO-d_6) 168.6 (*C*=O), 154.5, 148.6, 140.2, 137.3, 129.8, 126.2, 123.2, 116.2, 112.4; *m*/*z* (ESI$^-$) 188 ([M-H]$^-$); HRMS (ESI$^+$) $C_{10}H_8NO_3$, ([M+H]$^+$) requires 190.0499; found 190.0501.

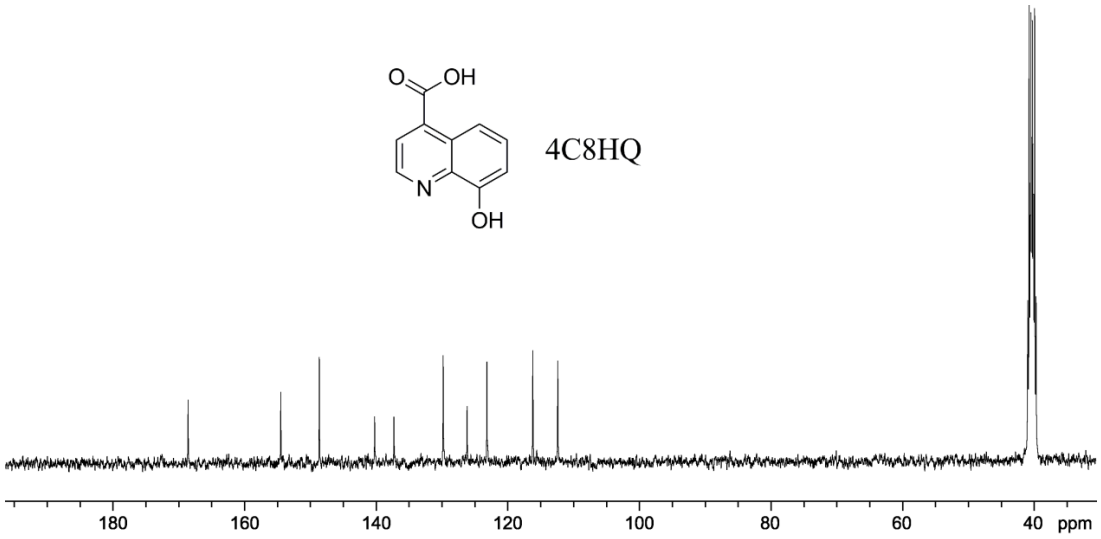

References

1. B. Yu and J. F. Hunt, *Proc. Nat. Acad. Sci.*, 2009, **106**, 14315-14320.
2. B. Yu, W. C. Edstrom, J. Benach, Y. Hamuro, P. C. Weber, B. R. Gibney and J. F. Hunt, *Nature*, 2006, **439**, 879-884.
3. C. G. Yang, C. Yi, E. M. Duguid, C. T. Sullivan, X. Jian, P. A. Rice and C. He, *Nature*, 2008, **452**, 961-965.
4. J. M. Elkins, K. S. Hewitson, L. A. McNeill, J. F. Seibel, I. Schlemminger, C. W. Pugh, P. J. Ratcliffe and C. J. Schofield, *J. Biol. Chem.* **2003,** 278, 1802.
5. M. A. McDonough, L. A. McNeill, M. Tilliet, C. A. Papamicaël, Q. Y. Chen, B. Banerji, K. S. Hewitson and C. J. Schofield, *J. Am. Chem. Soc.*, 2005, **127**, 7680-7681.
6. K. S. Hewitson, B. M. R. Liénard, M. A. McDonough, I. J. Clifton, D. Butler, A. S. Soares, N. J. Oldham, L. A. McNeill and C. J. Schofield, *J. Biol. Chem.*, 2007, **282**, 3293-3301.
7. A. Conejo-Garcia, M. A. McDonough, C. Loenarz, L. A. McNeill, K. S. Hewitson, W. Ge, B. M. R. Liénard, C. J. Schofield and I. J. Clifton, *Bioorg. Med. Chem. Lett.*, 2010, **20**, 6125-6128.
8. O. N. F. King, X. S. Li, M. Sakurai, A. Kawamura, N. R. Rose, S. S. Ng, A. M. Quinn, G. Rai, B. T. Mott, P. Beswick, R. J. Klose, U. Oppermann, A. Jadhav, T. D. Heightman, D. J. Maloney, C. J. Schofield and A. Simeonov, *PLoS ONE*, 2010, **5**, e15535.
9. S. S. Ng, K. L. Kavanagh, M. A. McDonough, D. Butler, E. S. Pilka, B. M. R. Liénard, J. E. Bray, P. Savitsky, O. Gileadi, F. von Delft, N. R. Rose, J. Offer, J. C. Scheinost, T. Borowski, M. Sundstrom, C. J. Schofield and U. Oppermann, *Nature*, 2007, **448**, 87-91.
10. J. F. Couture, E. Collazo, P. A. Ortiz-Tello, J. S. Brunzelle and R. C. Trievel, *Nat. Struct. Mol. Biol.*, 2007, **14**, 689-695.
11. Z. Chen, J. Zang, J. Kappler, X. Hong, F. Crawford, Q. Wang, F. Lan, C. Jiang, J. Whetstine, S. Dai, K. Hansen, Y. Shi and G. Zhang, *Proc. Nat. Acad. Sci.*, 2007, **104**, 10818-10823.
12. N. R, Rose, S. S. Ng, J. Mecinović, B. M. R. Liénard, S. H. Bello, Z. Sun, M. A. McDonough, U. Oppermann and C. J. Schofield, *J. Med. Chem.*, 2008, **51**, 7053-7056.
13. N. R. Rose, E. C. Woon, G. L. Kingham, O. N. F. King, J. Mecinović, I. J. Clifton, S. S. Ng, J. Talib-Hardy, U. Oppermann, M. A. McDonough and C. J. Schofield, *J. Med. Chem.*, 2010, **53**, 1810-1818.
14. L. Kruidenier, C. -W. Chung, Z. Cheng, J. Liddle, K. H. Che, G. Joberty, M. Bantscheff, C. Bountra, A. Bridges, H. Diallo, D. Eberhard, S. Hutchinson, E. Jones, R. Katso, M. Leveridge, P. K. Mander, J. Mosley, C. Ramirez-Molina, P. Rowland, C. J. Schofield, R. J. Sheppard, J. E. Smith, C. Swales, R. Tanner, P. Thomas, A. Tumber, G. Drewes, U. Oppermann, D. J. Patel, K. Lee and D. M. Wilson, *Nature*, 2012, **488**, 404-408.
15. Z. Otwinowski and W. Minor, *Meth. Enzymol.*, 1997, **276**, 307-326.
16. W. Kabsch, *Acta Crystallogr. D Biol. Crystallogr.*, 2010, **66**, 133-144.
17. P. Evans, *Acta Crystallogr. D Biol. Crystallogr.*, 2006, **62**, 72-82.
18. R. J. Read, J. L. Sussman, A. G. W. Leslie and H. R. Powell, *Evolv. Meth. Macromol. Crystallogr.*, 2007, **245**, 41-51.
19. D. Ehrismann, E. Flashman, D. N. Genn, N. Mathioudakis, K. S. Hewitson, P. J. Ratcliffe and C. J. Schofield, *Biochem. J.*, 2007, **401**, 227-234.
20. K. S. Hewitson, L. A. McNeill, M. V. Riordan, Y. M. Tian, A. N. Bullock, R. W. Welford, J. M. Elkins, N. J. Oldham, S. Bhattacharya, J. M. Gleadle, P. J. Ratcliffe, C. W. Pugh and C. J. Schofield, *J. Biol. Chem.*, 2002, **277**, 26351-26355.
21. L. Hillringhaus, W. W. Yue, N. R. Rose, S. S. Ng, C. Gileadi, C. Loenarz, S. H. Bello, J. E. Bray, C. J. Schofield and U. Oppermann, *J. Biol. Chem.*, 2011, **286**, 41616-41625.
22. N. R. Rose, E. C. Woon, A. Tumber, L. J. Walport, R. Chowdhury, X. S. Li, O. N. F. King, C. Lejeune, S. S. Ng, T. Krojer, M. C. Chan, A. M. Rydzik, R. J. Hopkinson, K. H. Che, M. Daniel, C. Strain-Damerell, C. Gileadi, G. T. Kochan, I. K. H. Leung, J. Dunford, K. K. Yeoh, P. J. Ratcliffe, N. Burgess-Brown, F. von Delft, S. Muller-Knapp, B. Marsden, P. E. Brennan, M. A. McDonough, U. Oppermann, R. J. Klose, C. J. Schofield and A. Kawamura, *J. Med. Chem.*, 2012, **55**, 6639-6643.

23. J. B. Kristensen, A. L. Nielsen, L. Jorgensen, L. H. Kristensen, C. Helgstrand, L. Juknaite, J. L. Kristensen, J. S. Kastrup, R. P. Clausen, L. Olsen and M. Gajhede, *FEBS Lett.*, 2011, **585**, 1951-1956.
24. D. Rotili, M. Altun, A. Kawamura, A. Wolf, R. Fischer, I. K. H. Leung, M. M. Mackeen, Y. M. Tian, P. J. Ratcliffe, A. Mai, B. M. Kessler and C. J. Schofield, *Chem. Biol.* 2011, **18**, 642-654.
25. E. C. Woon, M. Demetriades, E. A. Bagg, W. Aik, S. M. Krylova, J. H. Ma, M. Chan, L. J. Walport, D. W. Wegman, K. N. Dack, M. A. McDonough, S. N. Krylov and C. J. Schofield, *J. Med. Chem.*, 2012, **55**, 2173-2184.
26. I. K. H. Leung, T. Krojer, G. T. Kochan, L. Henry, F. von Delft, T. D. W. Claridge, U. Oppermann, M. A. McDonough and C. J. Schofield, *Chem. Biol.*, 2010, **17**, 1316-1324.
27. A. M. Rydzik, I. K. H. Leung, G. T. Kochan, A. Thalhammer, U. Opperman, T. D. W. Claridge and C. J. Schofield, *ChemBioChem*, 2012, **13**, 1559-1563.
28. A. Kawamura, A. Tumber, N. R. Rose, O. N. F. King, M. Daniel, U. Oppermann, T. D. Heightman and C. J. Schofield, *Anal. Biochem.*, 2010, **404**, 86-93.
29. A. J. McCoy, R. W. Grosse-Kunstleve, P. D. Adams, M. D. Winn, L. C. Storoni and R. J. Read, *J. Appl. Crystallogr.* **2007,** 40, 658.
30. P. D. Adams, P. V. Afonine, G. Bunkoczi, V. B. Chen, I. W. Davis, N. Echols, J. J. Headd, L. W. Hung, G. J. Kapral, R. W. Grosse-Kunstleve, A. J. McCoy, N. W. Moriarty, R. Oeffner, R. J. Read, D. C. Richardson, J. S. Richardson, T. C. Terwilliger, and P. H. Zwart, *Acta. Crystallogr. D Biol. Crystallogr.*, 2010, **66**, 213-221.
31. P. Emsley, B. Lohkamp, W. G. Scott and K. Cowtan, *Acta Crystallogr. D Biol. Crystallogr.* 2010, **66**, 486-501.
32. A. T. Brunger, P. D. Adams, G. M. Clore, W. L. DeLano, O. Gros, R. W. Grosse-Kunstleve, J. S. Jiang, J. Kuszewski, M. Nilges, N. S. Pannu, R. J. Read, L. M. Rice, T. Simonson and G. L. Warren, *Acta Crystallogr. D Biol. Crystallogr.*, 1998, **54**, 905-921.
33. V. B. Chen, W. B. Arendall 3rd, J. J. Headd, D. A. Keedy, R. M. Immormino, G. J. Kapral, L. W. Murray, J. S. Richardson and D. C. Richardson, *Acta Crystallogr. D Biol. Crystallogr.*, 2010, **66**, 12-21.
34. Y. Zhao and D. Truhlar, *Theor. Chem. Account.*, 2008, **120**, 215-241.
35. C. Lee, W. Yang, R. G. Parr, *Phys. Rev. B*, 1988, **37**, 785-789.
36. N. P. Blackledge, J. C. Zhou, M. Y. Tolstorukov, A. M. Farcas, P. J. Park and R. J. Klose, *Mol. Cell.*, 2010, **38**, 179-190.
37. C. J. Cunliffe, T. J. Franklin, N. J. Hales and G. B. Hill, *J. Med. Chem.*, 1992, **35**, 2652-2658.
38. M. M. Mackeen, H. B. Kramer, K. -H. Chang, R. J. Hopkinson, C. J. Schofield and B. M. Kessler, *J. Proteome Res.*, 2010, **9**, 4082-4092.